Journal of Sound and Vibration 330 (2011) 955–975

Contents lists available at ScienceDirect

Journal of Sound and Vibration

journal homepage: www.elsevier.com/locate/jsvi

Chaos in brake squeal noise

S. Oberst, J.C.S. Lai *

Acoustics & Vibration Unit, School of Engineering and Information Technology, The University of New South Wales at the Australian Defence Force Academy, Canberra, ACT 2600, Australia

ARTICLE INFO

Article history:
Received 11 January 2010
Received in revised form
3 September 2010
Accepted 9 September 2010
Handling Editor: H. Ouyang
Available online 12 October 2010

ABSTRACT

Brake squeal has become an increasing concern to the automotive industry because of warranty costs and the requirement for continued interior vehicle noise reduction. Most research has been directed to either analytical and experimental studies of brake squeal mechanisms or the prediction of brake squeal propensity using finite element methods. By comparison, there is a lack of systematic analysis of brake squeal data obtained from a noise dynamometer. It is well known that brake squeal is a nonlinear transient phenomenon and a number of studies using analytical and experimental models of brake systems (e.g., pin-on-disc) indicate that it could be treated as a chaotic phenomenon. Data obtained from a full brake system on a noise dynamometer were examined with nonlinear analysis techniques. The application of recurrence plots reveals chaotic structures even in noisy data from the squealing events. By separating the time series into different regimes, lower dimensional attractors are isolated and quantified by dynamic invariants such as correlation dimension estimates or Lyapunov exponents. Further analysis of the recurrence plot of squealing events by means of recurrence quantification analysis measures reveals different regimes of laminar and random behaviour, periodicity and chaos-forming recurrent transitions. These results help to classify brake squeal mechanisms and to enhance understanding of friction-related noise phenomena.

1. Introduction

In automotive industry brake squeal has become an important cost factor because of customer dissatisfaction. In North America, up to one billion dollars p.a. were spent on noise, vibration and harshness (NVH) issues [1] while friction material suppliers allocated more than half their budgets to deal with NVH problems [2]. According to a J.D. Power survey conducted in 2002, 60 percent of warranty claims concerning the brake corner are due to brake squeal [3]. Up to 5 percent of the USA's gross national product can be accounted for by losses due to friction and wear, which includes brake noise related problems [4]. Despite almost 80 years of research and a good deal of progress having been made, the underlying mechanisms of noise generation are still not fully understood. Recent reviews cover acoustics of friction [1], mechanisms of squeal [5] and the application of numerical methods such as the complex eigenvalue analysis (*CEA*) or the time domain analysis to study brake squeal propensity [6] and design in terms of structural vibrations [7]. As Oberst and Lai [8] have pointed out, most of the research undertaken over the last two decades has focused primarily on exploring the mechanism of brake squeal using simplified analytical models or applying the finite element method (FEM) complemented by experiments to determine unstable vibration modes in a brake system. It was stated that most likely, no complete and

* Corresponding author.
E-mail address: j.lai@adfa.edu.au (J.C.S. Lai).

0022-460X/$ - see front matter © 2010 Elsevier Ltd. All rights reserved.
doi:10.1016/j.jsv.2010.09.009

practical solution is in sight in the foreseeable future. Therefore, as was concluded in Hoffmann and Gaul [9], brake squeal as a friction-induced nonlinear and highly sensitive problem could probably only be solved by incorporating uncertainties in modelling even though the problem is deterministic.

Deterministic chaos as an *expression* of nonlinearity which is extremely sensitive to changes in initial conditions accounts for the loss of *long-term predictability* [10]. In an utmost stage a seemingly random behaviour can be observed (e.g., turbulence). A good introduction to chaos theory is presented by Schuster and Just [11] in which the four main routes to chaos are described: the Feigenbaum, the Manneville–Pomeau, the Ruelle–Takens–Newhouse and intermittency I–III routes to chaos. A handy definition of chaos is presented in Linz and Sprott [12]: Physical flows need to (i) form a strange attractor, with underlying non-periodic long time behaviour, (ii) have a sensitive dependence on initial conditions, (iii) have a dimension greater than two with (iv) some nonlinearity in the vector field.

Tables 1–5, containing 45 references since 1938, present a chronological overview about research work on friction oscillators, pin-on-disc systems, beam-on-disc systems and laboratory brake set-ups which indicate, that deterministic chaos is observed in these systems and that conventional methods do not provide adequate insight. The following main observations can be made by analysing the papers listed in Tables 1–5.

Chaos in simplified models: Analytical models listed in Table 1 are mostly 1-dof systems but display very rich nonlinear and chaotic behaviour. For the forced 1-dof dry friction oscillator, although it is governed by a second-order differential equation (see Eq. (A.1) in Appendix A), with displacement and velocity as state variables, a third state variable $2\pi ft$ arises from the sinusoidal driving force term [13,14], so that the system can only be fully described in a phase space dimension of at least 3. Further an additional equation (Eq. (A.2) in Appendix A) has to account for the beginning and end of slip. This equation allows switching between two systems of differential equations [15–18]. The evolution from periodic to quasi-periodic and finally chaotic regimes (i.e., from torus in phase space to intermittency and strange attractors) for a harmonically driven system has been discussed [19–21]. The one degree-of-freedom system of a dry friction oscillator represents a minimal model of a physical flow of a friction system able to exhibit exorbitant complexity studied by Popp and Stelter [19], Feeny and Moon [20,21] and later by Hinrichs et al. [22]. Shin et al. [23,24] showed that a forced 2-dof, dry friction analytical model with negative friction-velocity gradient characteristic developed chaotic pad motion when

Table 1
Works on *oscillators*.

Author	Approach	Findings
Popp and Stelter [19]	Analytical, 1-dof, (1990)	• Higher periodic motions • Intermittent and toroidal chaos
Feeny and Moon [20]	Analytical, 1-dof, (1992)	• Friction highly nonlinear • Known maps differ from chaotic models
Feeny and Moon [21]	Experimental and analytical, 1-dof, (1994)	• Mass overtakes belt (overshooting) • State variable friction law • Stick–slip attractors: same family
Hinrichs et al. [22]	Experimental and analytical, 1-dof, (1997)	• Rich bifurcational behaviour • Experimental results match well
Thomson [32]	Analytical, 1-dof, (1999)	• High-frequency external excitation can effectively cancel the effect of the negative friction-velocity curve
Feeny and Moon [59]	Experimental, 1-dof, (2000)	• Chaos controlled by *quenching stick–slip*
Shin et al. [23,24]	Analytical, 2-dof, (2002)	• Chaos in reduced order brake model • Pad and disc *couple in sliding* motion • Damping can have negative effects
Herve et al. [57,58]	Analytical 2-dof, (2009)	• Limit cycle and quasi-periodic motion • Destabilisation paradox • Iso-damping: max growth of amplitudes, but best configuration against instability • Gyroscopic effects are not negligible
Paliwal et al. [61]	Analytical, 2-dof, (2002)	• Very sensitive to coupling-stiffness • Instability increases limit cycle diameter
Popp [45]	Experimental and analytical, 1-dof, (2005)	• Bifurcation followed by mode coupling • Active control of self-excited vibrations
Hetzler et al. [62]	Analytical, 1-dof, (2007)	• *Hopf*-bifurcations in sliding friction • Basin of attraction inside limit cycle • Linear *CEA* does not consider limitation
Ouyang [63,64]	Analytical 4-dof, (2008/09)	• State-feedback control of vibration • Asymmetric system matrix challenging

Table 2
Works on *pin-on-disc/plate systems*.

Author	Approach	Findings
Bowden and Tabor [65]	Experimental (1938)	• *Stick–slip* on metal/metal contact • Friction is a *discontinuous* process
Bowden and Tabor [66]	Experimental (1942)	• Vibration signal *intermittent* with jerks • Velocity dependency of friction
Earles and Soar [67,68]	Experimental (1971/78)	• Confirmation of sprag-slip
Earles and Badi [69]	Experimental (1984)	• *Abrupt changes* in acceleration • Squeal fugitive and high sensitivity to parameters
Earles and Chambers [70]	Experimental (1987)	• Damping: instability remains • Nonlinear, fugitive character • Intuitive predictions impossible
Tworzydlo et al. [71]	Experimental and analytical (1999)	• Surface separations • Friction couples bending modes • Bifurcations • Harmonics due to limit cycles • Irregular bursts and surface damage • Frict. seizure: *extreme amplitudes*
Chen et al. [34]	Experimental	• Squeal but no mode coupling • Squeal: negative or positive friction-velocity curve
Chen and Zhou [36,50] Chen et al. [44]	Experimental (2007)	• Time delay between normal and friction force responsible for squeal • Squeal due to elastic vibration of friction system
Duffour and Woodhouse [72,73]	Analytical (2004)	• Instability boundaries extremely sensitive to damping • Negative gradient of $\mu(v_s)$ destabilizes
Duffour and Woodhouse [38]	Experimental and analytical (2007)	• High *capriciousness* • Linear theory detected 70 percent of squealing modes (*CEA*)
Butlin and Woodhouse [74]	Analytical (2009)	• System extremely sensitive to changes in parameters • Neglecting physical effects can give rise to faulty results • High sensitivity even at low modal amplitudes

Table 3
Works on *beam-on-disc* systems.

Author	Approach	Findings
Tarter [75]	Experimental (1983)	• Slotted rotor eliminates squeal • Pad material and geometry important
Suganami et al. [76]	Experimental (1998)	• Possible squeal due to in-plane vibrations
Akay et al. [77]	Experimental (2000)	• Coupling of parts (locking-in)
Tuchinda et al. [47]	Experimental (2001)	• Instability by locking pin and disc mode • Fulguration point (locking-out)
Baillet et al. [30]	Numerical (2005)	• Rotational speed <6 rev/min (≈ 0.7 km/h): stick–slip • 6–35 rev/min: stick–slip-separation • Over 35 rev/min(≈ 4.2 km/h): slip followed by separation

frequencies of the pad and the disc were close (see also [25]). They considered the size of the limit cycle more important than its existence.

Evolution in experimental set-ups: From Tables 2–5, a change in experimental set-ups of predominantly simplified brake systems can be observed. In the beginning, pin-on-disc test rigs were used, running at low velocity regimes: researchers were interested in stick–slip phenomena. Over the years, the focus of research changed to mechanisms from stick–slip then sprag-slip to binary flutter theory with mode coupling favoured by most researchers nowadays, necessitating the development of new experimental set-ups. The set-up of a pin-on-disc system changed to a beam-on-disc, which allows for elastic support and coupling with other components. In Tables 4 and 5, the laboratory brake (LB) and the tribobrake

Table 4
Works on *laboratory brake* (*LB*).

Author	Approach	Findings
Giannini and Sestieri [43]	Experimental and numerical (2006)	• Squeal developed between 5 and 30 rev/min ($\approx 0.57-3.42$ km/h) • Angle of attack: high-frequency squeal at 0°
Giannini et al. [26]	Experimental analytical (2006)	• Onset of squeal: linear methods • After limit cycle: nonlinear models • Feedback: coupling pad and rotor-motion
Gianinni and Massi [78]	Experimental and numerical (2008)	• Pad size changes split-mode frequency • Sine, cosine and rotating squeal • Rotating squeal higher nonlinearity
Massi and Giannini [56]	Experimental (2008)	• High pad pressure sensitivity of squeal • Squeal: high *quasi-random low frequency* content

Table 5
Works on *tribo brake* (*TB*).

Author	Approach	Findings
Massi [79,55] Massi et al. [55]	Experimental and numerical (2006)	• Low freq. modes: excited at negative angle • Squeal: phase difference of in- and out-of-plane direction • Squeal develops only in *right conditions* • Instability by higher modal damping (large tune-in range) • Tangential pad vibration couples with disc bending mode
Giannini et al. [54]	Experimental and numerical (2007)	• *Disc doublet modes* veer (travelling waves) • Extreme exfoliations and cracks (lining) • Coupling: pad-disc, support-disc squeal • Damping increases squeal propensity • Extreme exfoliations and cracks (lining)
Massi et al. [41]	Experimental and numerical (2007)	• Linear *CEA* over-predicts instabilities • Nonlinear simulation match experiments
Massi et al. [80]	Experimental and numerical (2008)	• Fatigue excitations: cracks within layers • Exfoliations: squeal and large amplitude vibrations

(TB) can be seen as a further development of the beam-on-disc set-up which allows a wider range of parameter variations under laboratory conditions. Real lining material with reduced dimensions was used. The TB is the successor of the LB and allows for investigating tribological/dynamic aspects due to contact conditions [26]. Both set-ups, the LB and the TB are so far used mainly to study the mechanism of mode coupling.

Stick–slip as the dominant mechanism in disc brake squeal seems to be abandoned, due to its required low relative velocity [27]. However, one has to be careful with conclusions concerning the validity of mechanisms, as squeal develops in a wide range of velocity regimes and different (unknown) nonlinearities are involved, such as local sticking and detachments of the contacting surfaces [28–30]. Another example is the negative friction-velocity characteristic, which is also a known destabilising mechanism [31–33]. By using a sinusoidally driven pin-on-plate apparatus, Chen et al. [34] found experimentally, that squeal can occur not only in regions of negative but also positive friction-velocity gradients. Further, the occurrence of squeal could not be attributed to modal coupling. Beloiu and Ibrahim [35] studied friction-induced noise both numerically and experimentally by analysing the friction force, normal force and vibrations in the frequency-time domain using discrete wavelet transform for a pad-on-disc system. They found that due to the time variation of the contact forces, the motion of disc and pad is intermittently modulated by low and high frequency oscillations. By interpreting squeal occurrence based on forces and vibrations, they found that squeal noise was accompanied by a larger mean value of the instantaneous friction coefficient. In 2007, Chen and Zhou [36] applied various time-frequency analysis techniques to analyse friction-induced vibrations obtained in a pin-on-plate test rig. They found that contrary to the expectations arising from mechanisms of the negative friction-velocity gradient and modal coupling, all vibrations are limited in magnitude by nonlinearity.

Nonlinearity: With the advent of sophisticated computer technology, FE methods are more often used in recent years by applying linear methods as the complex eigenvalue analysis (*CEA*) to full brake systems. However, it is well known that the ability of the complex eigenvalue method to predict brake squeal propensity is limited and needs in practice to be supplemented by extensive dynamometer tests [37]. Linear methods [38] like the *CEA* either underestimate [39,40] or overestimate [23,33] the number of unstable vibration modes. Massi et al. [41] investigated linear and nonlinear numerical methods in a laboratory brake. The *CEA* in their simulation was useful to detect the frequency where an instability might occur but to determine the strength of this instability, a nonlinear time domain analysis was necessary to estimate the size

of the limit cycle. It is unclear how nonlinear the behaviour of brake components is and how this nonlinearity influences the overall acoustic radiation properties (see also [42]). It is estimated that the onset of squeal happens in linear conditions and that nonlinearity stabilises the vibration amplitudes [43,44]. It has also been found that the development of brake squeal noise is related to *Andronov-Hopf*-bifurcations in the time domain which are sometimes detectable by *CEA* [39,45]. However, other bifurcations may be possible, such as for instance border collision bifurcations, which are already observed in analytical discontinuous systems [46].

In general, it is accepted that nonlinearity plays an important role in the generation of brake squeal (see for instance [47,34,30,43,26]) and nonlinear models are necessary to estimate the vibration amplitude after the onset of squeal. Only recently, nonlinearity and steady-state solutions of vibration signals of a pad-on-disc system exhibiting multi-instabilities have been numerically investigated by Coudeyras et al. [48,49]. For a reduced finite element model, they used a generalised constrained harmonic balance method to compute nonlinear periodic or pseudo-periodic responses but no chaotic solutions were presented.

As nonlinearity, specifically the lifting off of the pad is studied and found to have an amplitude limiting function [36,50,44]. The lift-off is also discussed in Hoffmann and Gaul [51] who found that an analytical 2-dof beam-on-disc (sprag-slip) model does not have a steady sliding state and hence always shows limit-cycle behaviour, however, strong the applied viscous damping is. Chen and Zhou [36] attributed the limitation of the vibration magnitude found in their experiments to friction-induced vibrations being bounded by limit cycles due to the system nonlinearity. They found further by conducting experiments and numerical simulations [50,44] that the contact separation between the two sliding surfaces is a main nonlinear factor causing the squealing vibration to be bounded. In addition, they experienced that the time delay between the varying normal force and the ensuing varying friction strongly influences squeal occurrence and proposed this as a new mechanism of brake squeal.

Important in the context of nonlinearity and modelling is also the function the friction coefficient takes. In Ouyang et al. [52], an analytical six degrees of freedom elastic slider on disc friction system is studied and stated to be non-smooth, hence nonlinear, as conditions responsible for behaviour of the slider depend on the motion of the system. Important is, that this even holds true for a constant friction coefficient. Mathematically, this nonlinearity is simply expressed by the directionality of the friction coefficient which is dependent on the velocity (see also [16]) and represents a switching mechanism. With their nonlinear model, Ouyang et al. [52] observed complex periodic and quasi-periodic vibrations of the pad and the disc. They found that in-plane stiffness of the slider is a critical factor in triggering instability, whereas transverse stiffness of disc or slider is stabilising. As the pressure is increased, the motion develops from periodic to quasi-periodic and more unstable.

Damping: Ouyang et al. [52] elaborated for an elastic slider on disc system, damping of disc or slider in the transverse direction stabilises unstable vibrations; although damping the slider in-plane reduces the magnitude of the vibration, it fails to stabilise unstable motions. They also found that an increase in rotating speed of the drive point can cause the system to destabilise. Shin et al. [23,24] have found that contrary to popular beliefs, increasing damping of either the pad or the disc alone can cause instability as also observed in [53,54]. Massi et al. [55] found that for their tribo brake (essentially a beam-on-disc set-up), a large modal damping can reduce the response of the damped mode and hence prevent its participation in squeal coupling. However, a highly damped mode has higher probability to couple with other modes close to its natural frequencies because its tune-in range becomes larger, resulting in a higher squeal propensity. In Massi and Giannini [56] non-uniform modal damping of two coalescing modes (*CEA*) has shown to be responsible for increased squeal propensity in a beam-on-disc system. They also found that a homogeneous damping distribution decreases the likelihood of a developing dynamic instability. Herve et al. [57] studied friction-induced instabilities in a 2-dof analytical model of an automotive clutch, by examining changes in instability boundaries due to interactions between structural proportional damping and gyroscopic effects. If the damping is non-evenly distributed, the gyroscopic effects interact with the damping of the system and cannot be neglected anymore. In [58] it was found, that an iso-distribution of damping is desirable in order to avoid destabilisation (see also [23,24,53,54]), but an iso-distribution is also the worst configuration of damping for reducing the amplitudes of self-excited vibrations. In their nonlinear analysis of the 2-dof analytical model, stable quasi-periodic and chaotic motions were observed, highlighting the complex effects which may be present in a real brake system.

Control of brake squeal: Of interest is also the control of vibrations due to friction-induced instabilities. For a harmonically driven analytical 1-dof dry friction oscillators, it has been found that quenching stick–slip vibrations can effectively eliminate destabilisation due to a negative friction-velocity characteristic [32]. Feeny and Moon [59] showed that chaos inherent to a stick–slip oscillator can be removed by applying high-frequency excitations. Active control by means of delayed feedback mechanism in controlling either the normal force or quenching with high-frequency dither [60] have been also applied successfully in both analytical and experimental models (see also [45]). However, active vibration control of brake squeal and its squeal propensity is still in its infancy stage.

Overall, terms such as for instance *irregular* [71], *fugitive* [69,70], *capricious* [38] or *quasi-random* [56] are used in Tables 2–5 which are not directly related to analytical models, to describe disc brake squeal's high sensitivity to changes in system parameters. These are characteristics which are also inherent properties of nonlinear and chaotic systems. Studies on brake squeal noise listed in Tables 1–5 are based on analysis of vibrations in mainly simplified analytical models of friction oscillators (Table 1) or simplified experimental systems such as pin-on-disc/plate, beam-on-disc and laboratory brakes (Tables 2–5). With a few exceptions such as [22–24], these studies do not consider friction-induced vibrations from

the perspective of deterministic chaos. As shown in Table 1, like many other studies of friction-induced instabilities, Shin et al. [23,24] only examined analytical 2-dof friction systems in the context of chaos. While Hinrichs et al. [22] used nonlinear analysis tools (such as phase space plots and Lyapunov exponents) to analyse the results of simulation and experiments, there are a number of limitations: (a) the model is only a pin-on-disc system; (b) only vibrations are considered although the manifestation of squeal is acoustic; and (c) bifurcations are illustrated but it is not clear whether other routes to chaos are possible for brake squeal especially for squeal in a full brake system.

To the authors' knowledge no experiment is known where deterministic chaos and its route have been identified in the *squeal noise* of a *full brake system*. The objective of this paper is, therefore, to close the gap between chaotic phenomena found in simplified analytical models or simplified experimental systems both investigated by means of structural vibrations and the true dynamics of squeal in terms of acoustics in a full commercial disc brake system. A second objective is to explore a different approach to conventional FE analysis in predicting brake squeal propensity by using the theory of nonlinear dynamics. Firstly, the measures used in nonlinear dynamics are introduced and applied to five analytical functions in order to illustrate their meanings. Then, a sinusoidally driven 1-dof friction oscillator is examined using a range of these measures and the different regimes of oscillations are classified based on the attractors revealed. With the insights obtained, nonlinear recurrence quantification analysis is applied for the first time to squeal data (sound pressure) of a full brake system obtained in an industrial brake dynamometer. The development of squeal is quantified using nonlinear dynamics theory and possible routes to chaos and hence squeal are identified.

2. Basic measures

Many quantitative measures are used for analysing nonlinear dynamics [81,82]. Most of these are indicators and provide an estimate of the predictability of the dynamic system based on the reconstructed system's trajectories in phase space. Some of the measures used in this study are listed in Table 6. For the analysis of time series experimental data, conventional delay embedding techniques according to Takens embedding theorems are used [83]. The embedding delay is estimated by the first minimum of the averaged auto-mutual information. By applying the embedding delay to the time series and by using the false nearest neighbour algorithm [84], the minimum embedding dimension is calculated, so that the solution trajectories in the phase space are unfolded from the attractor. Parameters such as the embedding delay and embedding dimension used to embed the time series to reconstruct the solution trajectories in the phase space are called

Table 6
Brief explanation of dynamic invariants [81] and recurrence quantification analysis (RQA) measures [82,90].

Measure	Description
Embedding delay τ	• Time delay applied to time series data for the reconstruction of the phase space of a dynamical system • Estimated with the algorithm of the averaged auto-mutual information from its first minimum
Embedding dimension m	• Gives the dimension of phase space • Estimated by false nearest neighbour algorithm
Correlation dimension D_2	• Derived from slope of correlation sum • Lower bound topological/fractal dimension
Correlation entropies h_2	• System complexity • Affinity of generating information
K-entropies K_2, K_1	• As lower bound related to sum of positive Lyapunov exponents
Maximal Lyapunov exponent L_{max}	• Exponential divergence/convergence of nearby points in phase space
Recurrence plot *RP*	• Evaluation of recurrent incidents • Non-stationary, periodic, chaotic states • Recurrence quantification analysis (RQA) based on RP
Recurrence rate *RR*	• Quantifies recurrent states • Random behaviour has low value • Corresponds to definition of correlation sum
L-entropy *ENTR*	• Average amount: information of diagonals • Decreasing: less diagonals
Average line length *LL*	• Average diagonal line length • Decreases: periods get in average shorter
Determinism *DET*	• Measures predictability • Relates to diagonal lines (non-tangential motion)
Laminarity *LAM*	• States which remain fairly constant • Relates to horizontal lines, thus tangential motion
Divergence *DIV*	• Decreases: periodic structures vanish • Related to a lower limit to the sum of positive Lyapunov exponents

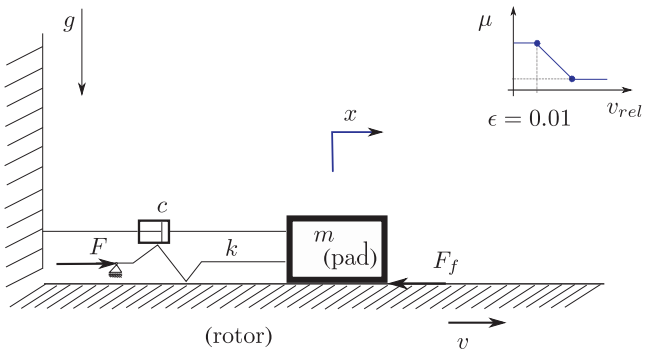

Fig. 1. Schematic of a friction oscillator [19].

embedding parameters [85]. One of the classic invariants as used in a metric analysis [86] to characterise a system is the correlation dimension. The correlation dimension is an estimate of the attractor's dimension which indicates fractality for non-integer values [87] and is calculated from a scaling region of the slope of the correlations sum [82]. Another classic invariant measure, the Lyapunov exponents, represents the rate of separation of the solution trajectories [88]. A positive Lyapunov exponent indicates exponential divergence of solution trajectories, hence sensitivity to initial conditions, which results in the loss of long-term predictability and fractal structures for the attractor [86]. Closely related are the *K*-entropy estimates, for which the sum of positive Lyapunov exponents defines an upper bound [89]. A positive entropy estimate, therefore, indicates chaos [82]. In time series analysis of nonlinear systems, recurrence plots are used to visualise the return of the solution trajectory in the phase space to a neighbourhood of a point of a previous state. The size of the neighbourhood is determined by a prescribed value of the parameter ε, hence this neighbourhood is referred to as the ε- neighbourhood. The recurrent states are expressed in a binary matrix with the value of 1 indicating the existence of a recurrent state and the value of 0 indicating the state is not recurrent [91]. Measures used in recurrence quantification analysis [85] listed in Table 6 are based on the statistics of recurrence plots and are used to quantify the dynamical behaviour of the system. The recurrence rate *RR* measures the percentage of recurrent states in a recurrence plot (laminar and deterministic states) [85] and corresponds to the correlation sum [82]. *ENTR* is the Shannon entropy of the probability distribution of all diagonal lines formed by ones in the binary matrix, whenever the distance between two points is found to be in the neighbourhood of a reference point. The shorter a diagonal line, the less information about the system's trajectory is included and hence the lower the value of entropy, indicating randomness. Determinism is the percentage recurrence rate for the diagonal lines in the recurrence plot and laminarity is percentage recurrence rate for the horizontal and/or vertical lines. The averaged line length *LL* is a measure to describe the evolution of the system states and is calculated from all the diagonal lines in the recurrence plot. A high value of the averaged line length implies long and stable periods while a low value of the averaged line length generally implies unstable or no periods. Divergence is the reciprocal value of the longest diagonal line length, corresponding to the longest period in the recurrence plot, and is related to the Kolmogorov–Sinai entropies (K_1, K_2), hence to the sum of the positive Lyapunov exponents [92]. A high value of divergence generally implies loss of stable periodic orbits. Consequently, an increasing divergence together with a decreasing average line length is an indication of a route to instability. Applications of these measures to analytical functions such as sinusoidal or logistic functions and the effect of noise can be found in [93,94]. The nonlinear dynamics of a forced 1-dof friction oscillator (Fig. 1) is chosen here as an example to illustrate the application of some of the measures (e.g., recurrence plots) given in Table 6 and to serve as a benchmark for comparisons with the analysis of real brake data in terms of the routes to chaos. The governing equations and detailed procedure in applying some of the measures in Table 6 are given in A.1. Results in Appendix A reveal three regimes: a limit cycle (one frequency); a weakly chaotic regime with a toroidal attractor (multiple distinct frequencies); and a broadband chaotic regime with the identification of the Ruelle–Takens–Newhouse route to chaos.

3. Experimental set-up

Measures described in Section 2 are applied to sound pressure signals obtained from a full front braking system of a midsize sedan with two-pistons and a floating fist calliper assembly. The brake system was tested in a computer-controlled industrial noise dynamometer of shaft type (LINK) [95] as part of a wider study described in more details by Moore et al. [96]. The calliper was made of cast aluminium, the bracket of spheroidal graphite cast iron, and the piston and the rotor of grey cast iron. The pads used in the production version of the brake system included chamfers and slots in the lining as well as a noise shim bonded to the back-plate of the pad. The pads used for the test did not have chamfers and any vertical slot, but noise shims. Noise shims are typically a metal-rubber laminate bonded to the pad back-plate and are therefore located between the piston or calliper housing and the pad's back-plate. Shims are very effective in improving the noise performance of a brake system [97]. Fig. 2(a) shows the computer-controlled chamber and the control unit. Fig. 2(b) shows

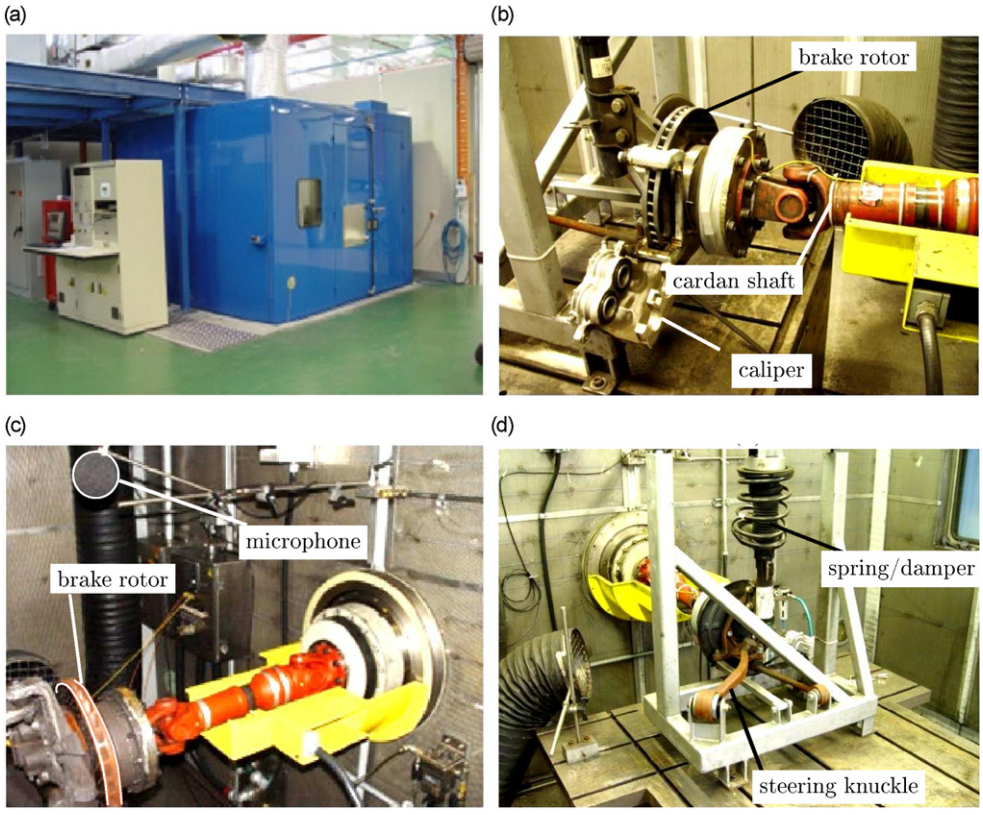

Fig. 2. Set-up of brake system on shaft dynamometer: (a) dynamometer chamber with control stand; (b) disc brake assembly fixed on hub and cardan joint; (c) brake rotor and microphone 0.5 m apart; (d) spring-damper (shock absorber) assembly with steering knuckle of a car's left front corner.

the inside of the dynamometer chamber, the brake disc bolted to a wheel adapter, drive plate and cardan drive shaft with the calliper housing flapped back for presentation purpose. Fig. 2(c) shows the microphone located at 0.5 m above the brake disc [98]. Fig. 2(d) shows the full set-up of a front braking system of a car's left corner, with steering control arms, bushes, shock absorber and spring, to provide boundary conditions representative of those on a car, with a cooling vent at the lower left corner. Pressure, velocity, initial humidity and temperature, were set to controlled values. After calibration and bedding-in brake applications, the pre-conditioned brake system was tested. In a sequence of 1669 stops, including forward/backward and warm/cold sections, squeal noise was recorded. The warm test matrix was conducted according to specification SAE J2521 [98], while the cold section was adapted to NVH customer specifications. The microphone's sampling rate was set to 44.2 kHz. Brake stops were ranked according to their highest sound pressure peak level. The top 20 stops were examined by analysing their time series, distance plots and spectrograms. Squeal phenomena found were quite different and time series with short squeaking events were discarded. In the end, eight events of 1669 stops with relatively long and constant squeals were found to exhibit similar behaviour. All of these stops were forward drag-stops in the cold section with a brake temperature near 0 °C and a rather constant velocity of around 40.5–41.0 rev/min ($\approx$4.8 km/h). Fig. 3 displays the initial brake temperature and humidity for the warm and cold sections recorded for each brake stop. It can be seen that the chamber temperature was kept rather constant by the computer control, but that, according to test specifications, the initial brake temperature varied significantly with stops. The humidity was not measured properly in the cold section due to a malfunctioning of the sensors at temperatures below 0 °C and was henceforth removed. From the sound files recorded using the microphone, only two examples are presented, each for a different case their position in the test matrix indicated in Fig. 3 by A and B. Case A is often observed in the eight brake stops and depicts the formation from a fixed point, over a limit cycle with tonal squeal frequency, to an unstable torus-like structure. This route to aperiodicity is typically observed and detectable by means of recurrence quantification measures. Case B provides evidence that not only the route to instability is relevant to brake squeal, but that the formation of a strange attractor with a more pronounced chaotic regime is possible. The route to this attractor is observed either over a torus or immediately over a limit cycle. Normalised brake-line pressure, rotational speed, μ and rotor temperature recorded at a sampling rate of 50 Hz for the two sample brake stops are shown in Fig. 4. These parameters are considered to be highly influential for brake squeal and may be treated as bifurcation parameters. The rotational release speed for the stops was about 4.8 km/h ($\approx$40.5 rev/min). The mean brake-line pressure was around 8 bar, the initial rotor temperature

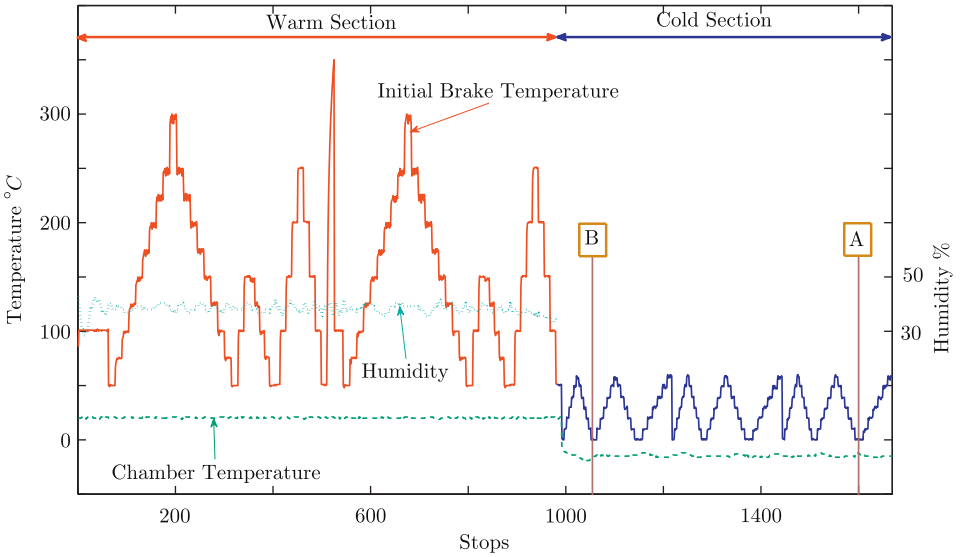

Fig. 3. Operating conditions recorded over the whole test matrix.

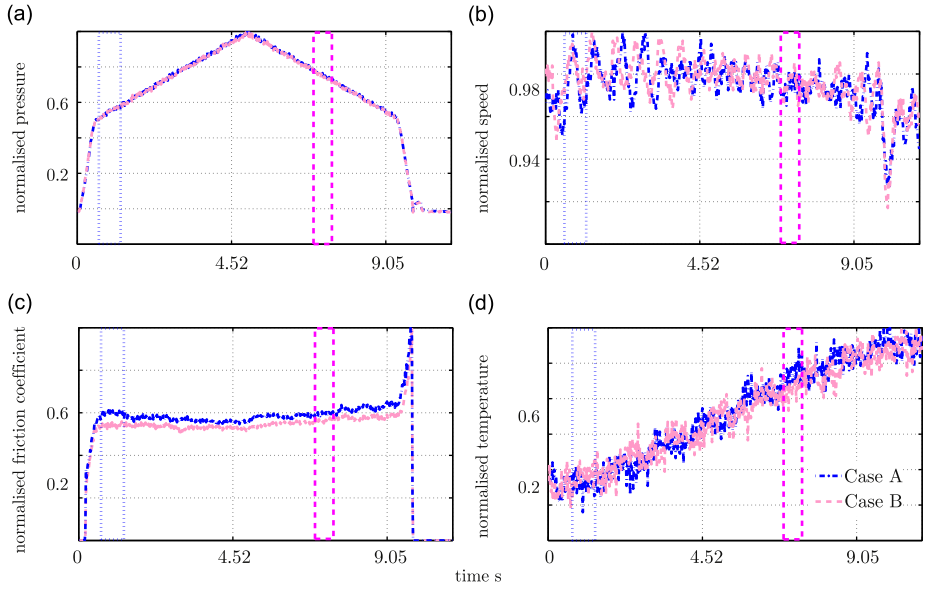

Fig. 4. Time traces of (a) brake-line pressure; (b) rotational speed; (c) friction coefficient; (d) rotor temperature for case A (···) and case B (—).

was between 276 and 278 K and normalised μ was on average 0.56 (0.378 not normalised) in case A and 0.60 in case B (0.416 not normalised). In most sound files investigated the value of divergence started to peak with decreasing velocity, hence for the friction model described in Section 2, the belt's velocity was the chosen bifurcation parameter. RQA is applied to the whole time series using a window of size 99 and a shift of one to allow the capture of fine structures. A larger window would smear short and important signals making it difficult to detect either chaos or its onset. For the RQA, embedding parameters $\tau = 1$ and m=5 were chosen [99]. The value of ε- neighbourhood was calculated as the ratio of the calibration signals standard deviation to the squeal's standard deviation and has been found to be 0.067 (case A) and 0.056 (case B), which was smaller than 10 percent of the maximum phase space diameter (case A: 0.071, case B: 0.062) [82,94,90].

4. Analysis of brake squeal time series data—case A

At first the recurrence quantification analysis (RQA) measures are applied to the time signal. Fig. 5(a) displays the time series of the sound pressure signal for the whole time series together with three measures: determinism/recurrence rate

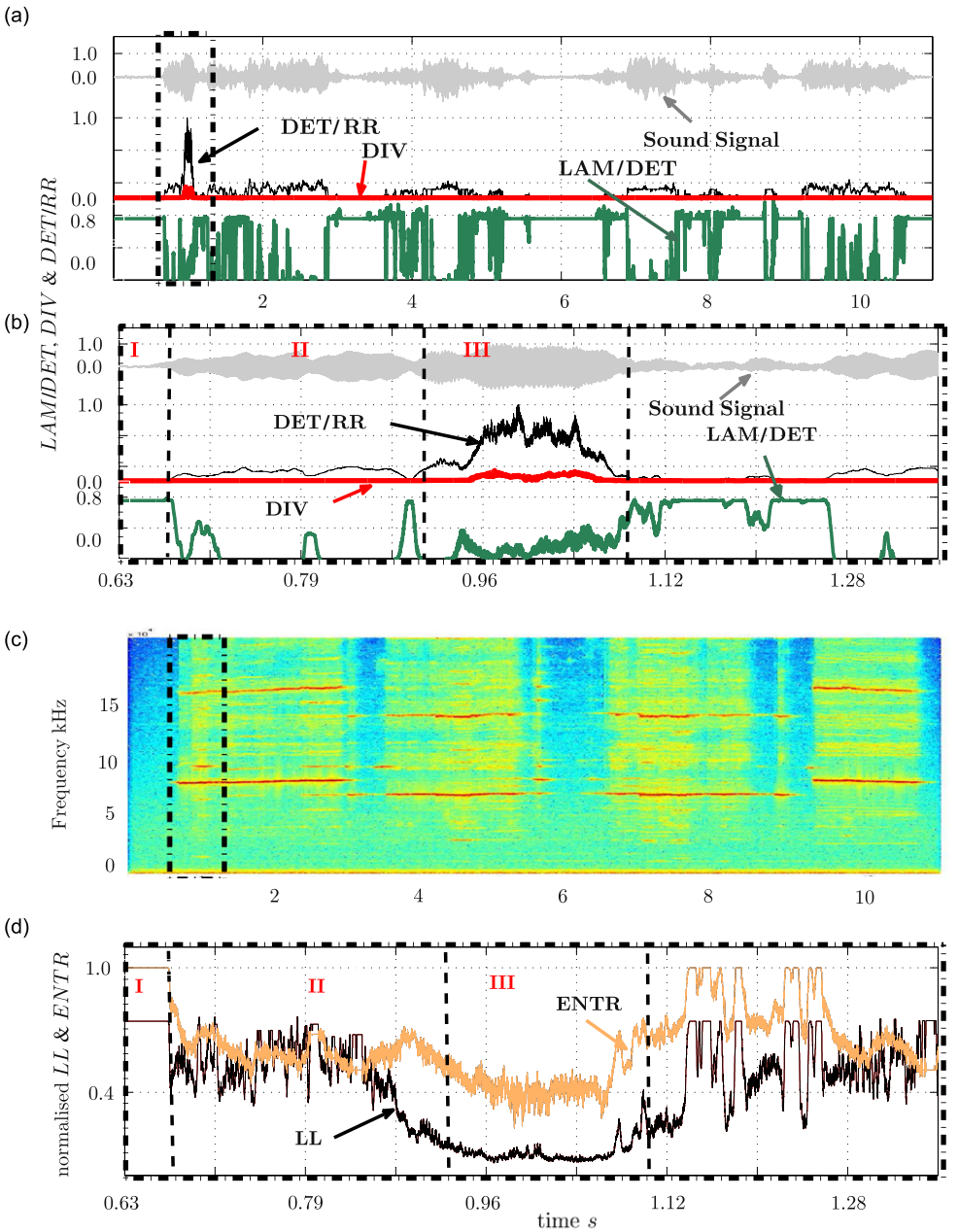

Fig. 5. Case A: (a) sound pressure signal, DET/RR, LAM/DET and DIV; (b) boxed area magnified; (c) spectrogram; (d) average line length (LL) and entropy of diagonal lines (ENTR).

(*DET*/*RR*), laminarity/determinism (*LAM*/*DET*) and divergence (*DIV*). A section of the whole time series was extracted to form case A (i.e., 0.63–1.31 s) displayed in Fig. 5(b). Fig. 5(c) displays the spectrogram obtained for the whole time series in Fig. 5(a). Signals of additional measures (normalised average line length of diagonal lines (*LL*) and normalised entropy (*ENTR*)) corresponding to Fig. 5(a) are shown in Fig. 5(d). In a second step classic dynamic invariants will be presented.

4.1. Recurrence quantification analysis

Zone I : Fig. 5(a) indicates high *LAM* compared with *DET*. Laminar states can be seen in the corresponding RP in Fig. 6(a) and (b) in which more vertical and horizontal lines are present than isolated diagonal line structures before a transition to a limit-cycle regime appear. In Fig. 6(a), the segment from 0.34 to 0.45 s shows an auto-regressive process [90] before contact between the brake pad and rotor is fully established and squeal has not developed yet, which is confirmed by the spectrogram in Fig. 5(c) and its power spectral density (PSD) in Fig. 7(a). This state corresponds to a stable fixed point

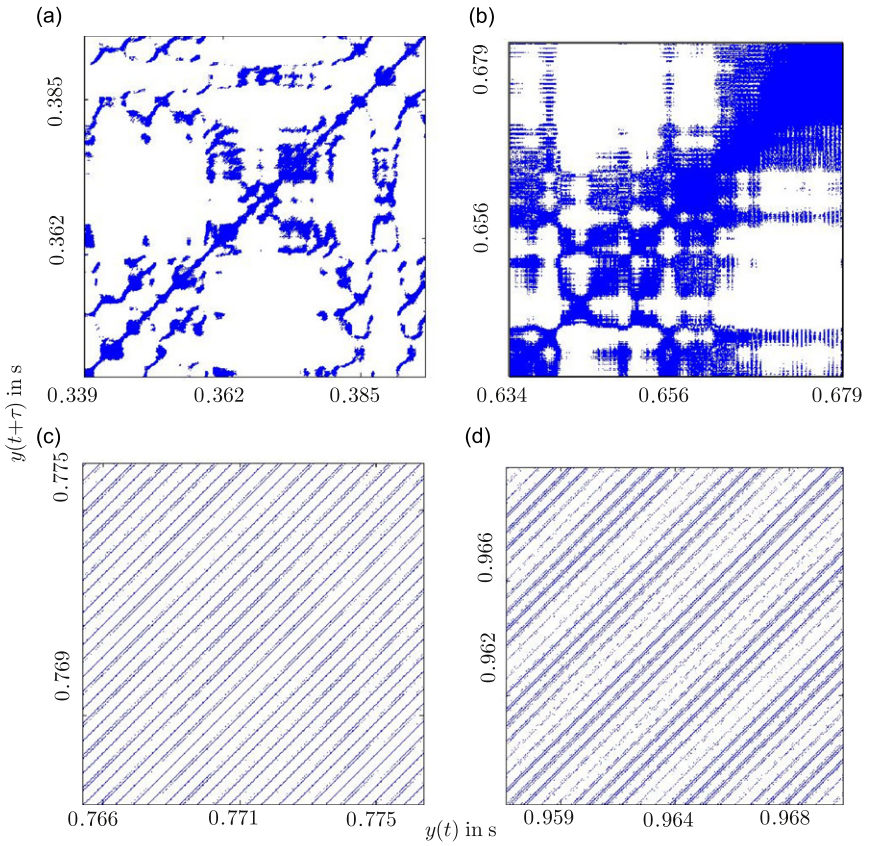

Fig. 6. RPs case A: (a) auto-regressive pre-squeal regime; (b) Zone I, transition to limit cycle; (c) Zone II, limit cycle/torus regime; (d) Zone III, unstable torus.

which is depicted in Fig. 7(a) in the first column. The system's evolving trajectory is captured in a state of very little change (laminar), rather than evolving (as expressed by *DET*). At the beginning of the brake stop no distinct frequency apart from a broadband spectrum can be seen (Fig. 7(a)). Three zones are identified in the magnified interval (Fig. 5(b)) with their corresponding *RPs* in Fig. 6. Fig. 6(b) depicts the RP of a transition from an unstable fixed point to a limit cycle, as shown in the phase space plot of Fig. 7(b), and represents zone I. This system behaviour is due to supercritical Andronov-Hopf-bifurcations [45,11]. The black region in the upper right corner of the RP in Fig. 6(b) corresponds to already limit-cycle behaviour with a high value of *DET*. As soon as the amplitudes of the time series increase (Fig. 5(a) and (b)), the spectrogram becomes richer and distinct frequencies appear (Fig. 5(c)). These frequencies indicate the tonal character of squeal noise.

Zone II : As soon as zone II is approached, the fundamental frequency and its harmonic (8.475 and 16.95 kHz) appear in the PSD (Fig. 7(b) and (c)). This indicates the birth of a limit cycle as depicted in Fig. 7(b) leading to (c). This transition to zone II is accompanied by a drop in *LAM*/*DET*, whereas at the same time, the ratio of *DET*/*RR* increases slightly (Fig. 5(b)). This is an effect of the shrinking value of the RR whereby the system's behaviour becomes more complex. *DET*, as well as a low *LAM*, indicates that a recurrent signal is present which gives unbroken, diagonal lines in the RP in Fig. 6(c). In the limit-cycle regime, transitions between two periodic-like regimes occur and are marked by a maximum in *LAM* at 0.79 s (Fig. 5(b)). These transitions are called period-period transitions and, finally marked by bifurcations, they initiate the formation of a torus [11], as shown in Fig. 7(d).

Zone III : The divergence *DIV*, which is the reciprocal value of the maximum diagonal line length in the window of interest, with a rather constant and low value in zone I and II, starts to increase (Fig. 5(b)). If the value of the maximum line length approaches zero, periods are getting disrupted, thereby indicating chaos. However, as changes in the *DIV* simply show that the diagonal line structures in the RP become more complicated, it is necessary to be careful about drawing definite conclusions. If other measures do not show behaviour usually encountered in unstable becoming systems, the torus will only get more complicated, more modes will be involved and the system will merely remain quasi-periodic; for example, in zone III, at 10.5 kHz, the second harmonic becomes distinguishable (Fig. 7(d)). This corresponds to a so-called *secondary Hopf*-bifurcation, which can follow after a limit cycle [11]. Further, it is observed that *LAM* in zone III increases slightly and that fluctuations might indicate the instability of the attractor. Also, the value of the *LL* drops as well as the *ENTR* (Fig. 5(d)). The transition to a state of higher energy is indicated by a maximum in *LAM*/*DET* after which the *DIV*

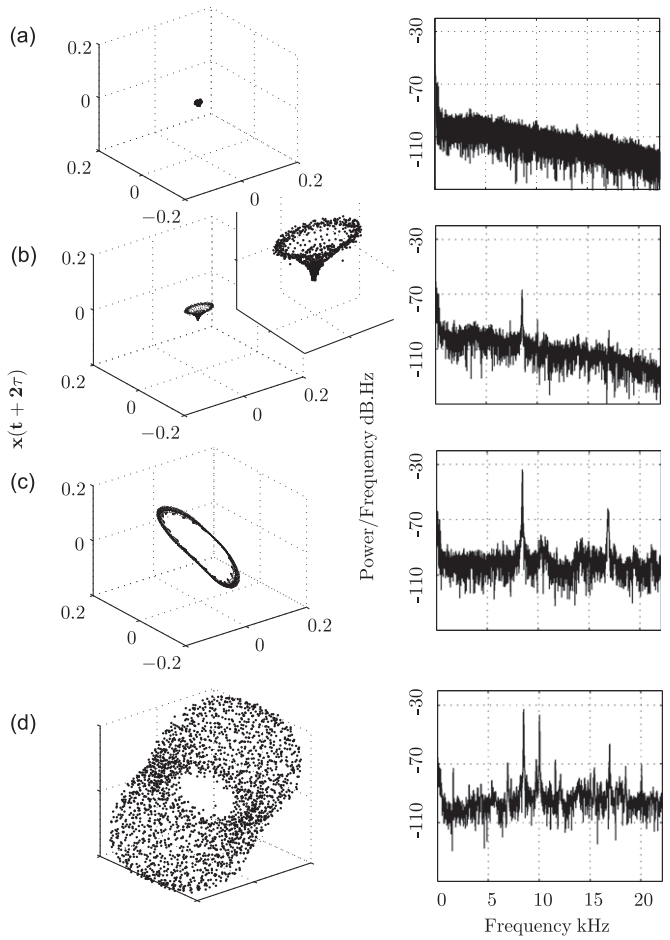

Fig. 7. Power spectral density (PSD) case A: (a) Zone I, transition to limit cycle; (b) Zone I, forming limit cycle (vortex); (c) Zone II, limit cycle; (d) Zone III, (chaotic) torus attractors for case A.

increases. In the first part of zone III, a torus is formed (Fig. 7(d)). The steep increase in the measure *DET*/*RR* initiates the upcoming chaotic regime in which the maximum length of the diagonal lines decreases significantly; the *DIV* becomes almost 5 percent in comparison to approximately 0.1 percent previously (Fig. 5(b)). The RQA measures in Fig. 5(b) show that the RR decreases but *DET*, which indicates the system's predictability, does not decrease at the same rate. The spectrogram shows an increase in the frequencies involved (Fig. 5(c)) while the PSD indicates a broadband characteristic which is slightly lifted up (Fig. 7(d)). Although *DET*/*RR* drops abruptly as the system loses its stability, it increases again when a chaotic regime is approached. *LAM* becomes lower in comparison with the system's *DET*. An important measure, which must always be considered, is *LL* (Fig. 5(d)). If only *DIV* becomes high, without a corresponding decrease of *LL*, then chaos could not be detected in the experiments. The PSD in Fig. 7(d) displays more distinct frequencies and is more broadband in nature but obviously not turbulent, yet. After the *DIV* returns to a lower value similar to that in zones I and II, a new cycle is initiated except that, in the audible range, the squeal does not vanish. This is confirmed by one major squeal frequency and its harmonic in the spectrogram (Fig. 5(c)). Clearly, the phase space dimension of the attractor has grown, indicating that the torus underlying dynamics (Fig. 7(d)) radiate at a higher sound pressure level than does the limit cycle.

4.2. Dynamic invariants

Table 7 provides an overview of the attractor's invariant estimates in the three zones. In order to interpret these attractors, the dynamic invariants D_2, K_2, K_1 and h_2, as well as $L_{\max}$ given in Table 6, have been calculated and are listed in Table 7 using the TISEAN software package [100]. The invariant measures were calculated for the described zones of the sound pressure signal firstly without and then with nonlinear filtering [101,102] to reduce the effects of noise in the data. In case A, the development towards chaos from zones I to III is evident as the D_2 estimate increases until it becomes a non-integer and fractal. It was found that the D_2 of zone I approaches zero as a fixed point with the dimension of zero in the phase space. Reasons for this value being not exactly zero are: experimental data are always noisy despite this data set

Table 7
Parameters and dynamic invariants.

Case	Zone	Interval (s)	τ	m	D_2	K_2	K_1	h_2	L_{max}
A	*I*	0.67–0.72	2	2	0.1	0.014	0.0298	0.000	−0.070
	II	0.72–0.81	1	3	1.0	0.003	0.0099	0.012	0.006
	III	0.94–1.02	15	4	2.6	0.478	0.3790	0.174	0.147
B	*III*	7.53–7.62	50	5	2.2	0.42	0.3125	0.15	0.175

Time delay τ, embedding dimension m, correlation dimension D_2, K—entropies K_1, K_2, correlation entropy h_2, maximal Lyapunov exponent L_{max}.

being de-noised with nonlinear filtering; the sequences chosen are finite, here using the interval 0.63–0.72 s; and zone I represents a transitional regime from a fixed point to a limit cycle. D_2 for zone II has an obvious scaling behaviour for many different embedding dimensions around the integer value of one, indicating a limit cycle and the absence of fractality. In zone III, D_2 is about 2.5 which indicates fractality. Since a non-integer dimension can be due to fractality, which is a by-product of the stretching and folding process of the attracting sub-set, the attractor in Fig. 7(d) is very likely to lie somewhat close to a torus dimension of $D_2=2$ in order to fit into the prescribed phase space dimension. The K-entropies are non-zero, hence the sum of the positive Lyapunov exponents is greater than zero. L_{max} was calculated and if positive, is a typical sign of chaos since the trajectories no longer exhibit volume-preserving behaviour and diverge. For the point attractor in zone I, the characteristic Lyapunov exponent is negative while, for the limit cycle in zone II, it is near zero and, for the unstable torus-like structure in zone III, L_{max} is positive.

5. Analysis of brake squeal time series data—case B

Case B illustrates the route to chaos and also the formation of a strange attractor apparently not related to a typical quasi-periodic torus structure. Fig. 8(a) displays the time series of the sound pressure signal for the whole time series, together with three different measures: *DET*/*RR*, *LAM*/*DET* and *DIV*. A section of the whole time series is extracted to form case B (i.e., 7.31–7.62 s samples), as displayed in Fig. 8(b). Fig. 8(c) and (d) displays the corresponding spectrogram and time series of normalised *LL* and *ENTR*. Similar to case A, three zones are identified in Fig. 8(b). Zones I and II in case B behave mostly in a similar fashion to those in case A. Therefore, only zone III is investigated in detail in the following in order to explore whether a *strange* attractor exists.

5.1. Recurrence quantification analysis

Zone I : After an epoch of high *LAM* this measure drops before a sequence of periodic-like behaviour follows (Fig. 8(b)). Zones I and II are in this case rather short, the limit cycle changes directly into a chaotic regime. In comparison with the brake stop in case A, the spectrogram in Fig. 8(c) shows many more distinct frequencies. *LL* and *ENTR* remain at high and constant values (Fig. 8(d)).

Zone II : The *LAM* diminishes and *DET*/*RR* increases while the *DIV* does not show any particular change. Shortly before zone III begins, *LAM* reveals a local maximum, indicating a transition from periodicity to chaos. At the same time, *DET*/*RR* shows a minimum but rises afterwards to a slightly higher level. The *LL* and *ENTR* based on diagonal lines start oscillating and then decrease in their overall level.

Zone III : High values of *DIV* can be observed while the *LL* decreases. *DIV* reaches values from 10 percent up to 53 percent (Fig. 8(b)). The distinct peaks in *LAM* reveal that while the system is in the chaotic regime, chaos/chaos transitions occur [99,103]. In Fig. 9(b) and (c) the attractor and the RP for zone III are given. The RP in Fig. 9(c) now shows broken and irregular lines evidently due to deterministic chaos. A sudden drop of *LL* and *ENTR* can be observed (Fig. 8(d)).

5.2. Dynamic invariants

The calculated dynamic invariants are given in Table 7, clearly indicating the presence of chaos. The estimates for the PSD in zone III is depicted in Fig. 9(a). In comparison to the PSD of case A in (Fig. 7(d)), evidently more frequencies are involved and the spectrum is more broadband. The correlation dimension D_2 is estimated to be 2.2. The attractor in Fig. 9(b) is plotted in a folded state, whereas in Fig. 10 the unfolded attractor is presented. Fractality is due to the basic operations stretching and rotation (linear) and folding (nonlinear).

6. Discussions

Real-life brake squeal data presented here indicate that when conditions for chaos are established, the brake system squeals. Thus, a qualitative definition of the route to chaos in brake squeal can be provided here in terms of RQA, as illustrated in Table 8. The first row of the matrix is set to be the initial state to which the second row is related to. The third row expresses the system's development in relation to the second row, etc. The signs "+/−" indicate increasing/decreasing

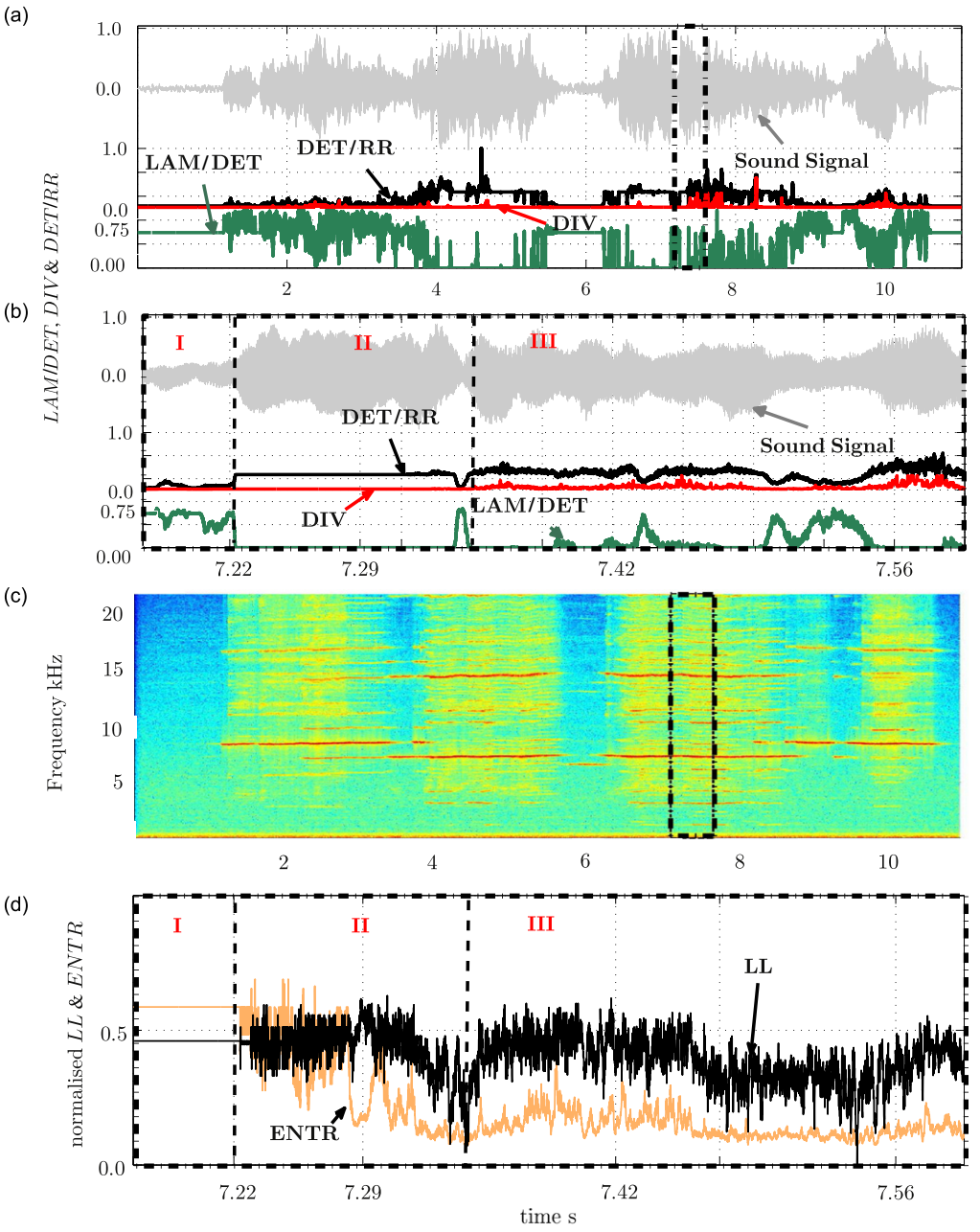

Fig. 8. Time series for case B: (a) microphone signal, *DET*/*RR*, *LAM*/*DET* and *DIV*; (b) magnified interval indicated by dashed square in (a); (c) spectrogram; (d) entropy (ENTR) and average line length (LL).

values relative to the previous row. Double signs, such as "==", indicate that the system's behaviour is almost constant, whereas "++" represents a strong increase. A "(*c*)" is the placeholder for a constant and "−(*c*)" means that the measure, as it decreases, is then almost constant in this segment. The route to chaos described consists of a section with high *LAM* followed by a section with high *DET* and a drop in *LAM*, and a third section with high *DIV*, low *LL* where more frequencies become involved. However, no bifurcation diagram could be obtained because the control parameters could not be held constant, even in a computer-controlled dynamometer test rig. Also, it is not sure if the attractors found are codimension-1 attractors or if a combination of several control parameters is necessary to induce bifurcating behaviour. It was observed in the existing data, that usually a fixed point leads to a limit cycle which develops into an (unstable) torus leading to louder sound pressure amplitudes. A torus regime could be found quite often although, when the *DIV* increases, very quickly strange attractors were established. The formation of an attractor, whether strange or not, is indicated by the RQA with a local minimum in *DET*/*RR* and a local maximum in *LAM*/*DET*. As some of these transitions correspond to bifurcations, more

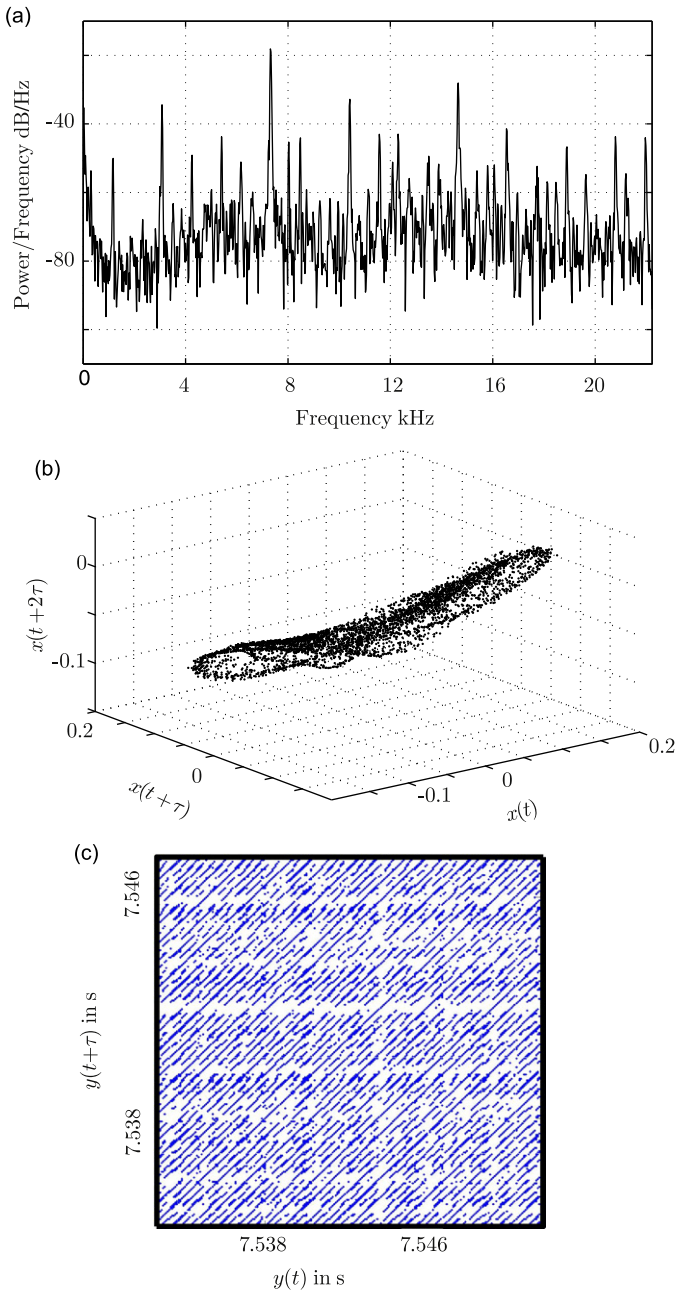

Fig. 9. Chaotic regime case B: (a) PSD; (b) phase space plot; (c) recurrence plot.

frequencies in the PSD are observed. Further, the spectrogram shows different frequencies at different times and may be used to locate bifurcations. Bursts of chaos can be seen in Fig. 8(a) and (b), as indicated by sudden increases in the *DIV*. It is clear from Fig. 8 that chaos (typified by high *DIV*) does not always coincide with the highest sound pressure amplitude. Nevertheless, case A is archetypical since, in most cases, very severe and high squealing amplitudes are observed in the regimes of high *DIV*, for example, as depicted in Fig. 5(a) and (b). One type of chaos in brake squeal, zone III, can be defined as the part of the time series of the sound pressure signal in which high *DIV*, a medium level of *DET*, a low *RR*, low *LAM*, low *ENTR* exist, when initiated by a significant increase then constant *LAM*/*DET*, and a decrease in *LL*. The classical invariants show that, where the torus structure is formed, the system already behaves in an unpredictable fashion (see K_2-, K_1-, L_{max}-estimates) even when the PSD is not lifted up significantly relative to the previous limit cycle regime and does not show many distinct frequencies. The process of stretching, rotation and folding has already started. However, it is important to note that chaos is not a pre-requisite for squeal. Brake squeal is able to be detected and predicted in some cases by means

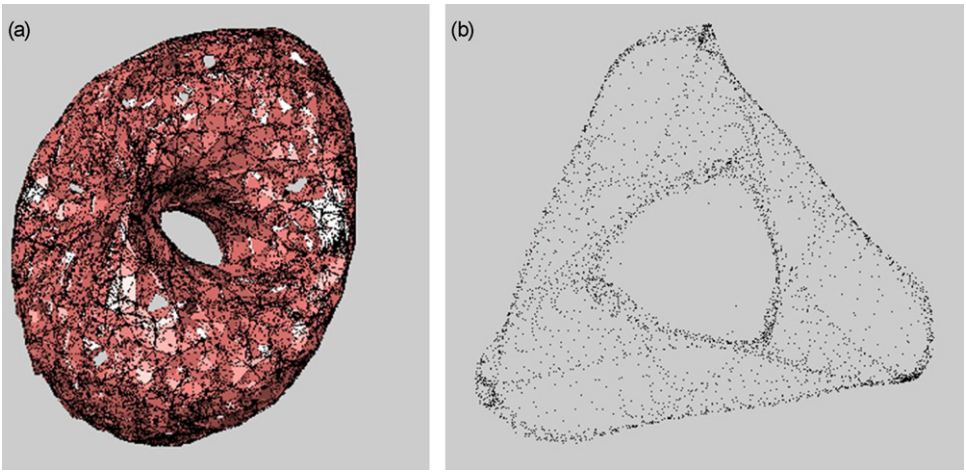

Fig. 10. Attractors zone III: (a) case A; (b) case B.

Table 8
The table shows the trends of the brake system's dynamics, in terms of RQA measures.

Transitions	*RR*	*LAM*	*DET*	*LL*	*DIV*	*ENT*	Squeal	# freq.
I (initially)	**high**	**High**	**High**	**High**	**Low**	**High**	**No**	**Low**
I→*II*	−	− −(c)	+(c)	+(c)	=	= −(c)	Yes	+
II→*III*	−	=+	−	− −	++	−	Yes	++
III→*I*	++	++	+	++	− −	+	no	− −

The signs −,=,+ indicate the rate of change relative to a previous regime.

of linear methods, for instance, by the complex eigenvalue analysis. This is due to the centre manifold theorem which analyses the dynamical system around its linearised equilibrium [104]. Brake squeal can start with an instability indicated by an *Andronov-Hopf*-bifurcation [95,45], then it might proceeds in nonlinear conditions [41]. Evidently, chaos is due to existing nonlinearity which dominates the system behaviour in these regimes and starts with an audible transition from a fixed point to a limit cycle. However, researchers of disc brake squeal usually focus and discuss only the limit-cycle phenomenon rather than the route towards instability which is investigated here. It is found that the actual limit-cycle regime is never purely present for a long time but that transitional states, for example, between the limit-cycle regime and the torus, are the attractors most often encountered. Furthermore, a regime may not look turbulent, however, the long time predictability might already be lost (positive Lyanpunov exponent), hence this regime has to be called chaotic. Also, broadband spectra similar to turbulence often cannot be observed while some frequencies remain quite distinct. This is consistent with a system behaving in a weakly chaotic (*non-turbulent*) fashion [11]. Therefore, it seems necessary to distinguish between weak chaos (no real broadband spectrum), chaos (broadband spectrum, where one Lyapunov exponent becomes positive), and stronger chaos (hyper-chaos up to turbulence) where the trajectory is diverging in more than one direction [105].

In case B, distinct frequencies are still visible although the PSD function in Fig. 9(a) clearly shows that the number of modes involved has significantly increased. For the time interval chosen (7.24–7.81 s), the formation of a torus has not been observed as the strange attractor is formed directly after the limit-cycle regime. Similarly, in Feeny and Moon [21], the route to chaos through bifurcations was also not observed in a dry friction 1-dof oscillator. They assumed that the system becomes unstable in such a very short time that these bifurcations are simply not observable. This is consistent with the description of the Ruelle–Takens–Newhouse route to chaos [11] and is also confirmed in case B. However, in other parts of the time same series the formation of the torus was observed. Another possibility is the formation of border collision bifurcations from a limit cycle directly into chaos which were already evidenced in discontinuous dynamical systems [46]. The attractor in case B was found and formed whenever the recurrence quantification measures indicated instability but also vanished after some time. If present for a longer period, it rotated in phase space initiated by (a) varying operation conditions which trigger a (b) change in embedding parameters. This indicates that the geometric structure formed by chaos is in itself quite robust (attracting); however, to investigate longer time series of the attractor, a continuous synchronisation technique of dynamic regimes is necessary [103,94]. Further, even in the chaotic regime, squeal remains tonal and clearly audible. This indicates that deterministic chaos does not have to sound and act like white noise. However, in the present brake squeal data, several control parameters (such as temperature, stiffness, friction coefficient, brake-line pressure and rotor speed) change continuously with time. Even when the attractor in zone III in case

B is found in the whole section (7.24–7.81 s), it was not possible to enlarge the basis for one calculation by using the whole section of sample points. Changes in the system's characteristics make it almost impossible to capture a regime long enough to enable the extraction of detailed features of the chaotic attractor. Also, the effects of noise need to be considered in a constantly changing system with unsteady bifurcation parameters as they make capturing a long stationary state very difficult. Only quasi-stationary regimes are chosen with the help of distance plots, *RPs* and their quantification measures. Owing to changing parameters, chaotic attractors cannot be observed with more data points without phase space synchronisation even if the same mechanism was at work as indicated by the same geometry of the strange attractor.

7. Conclusions

By using traditional invariant measures used for nonlinear dynamics analysis, a sinusoidally driven 1-dof friction oscillator, with relative velocity as control parameter, has been shown to exemplify the transition from a limit cycle over a torus to a chaotic attractor. Then, similar quantitative analysis and for the first time recurrence quantification analysis were applied to brake squeal data obtained by a single microphone in a full brake system tested in an industrial dynamometer. Despite the poor signal to noise ratio in the brake squeal microphone data and varying parameters, a number of dynamic regimes of interest have been identified as transiting from a limit cycle to an unstable torus attractor which is very similar to the behaviour of the single dof friction oscillator. Further, it is the first time that a qualitative correlation between nonlinear dynamics theory (chaos) and real-life brake squeal data has been established. Preliminary numerical simulation studies of a pad-on-disc system using sound pressure data show similar chaotic phenomenon to that observed here [106,107]. Further, the *route* to chaos confirms the *developing character* of squeal [55,41] and more routes are likely. Also, it should be noted that chaos is not the only mechanism for brake squeal generation. However, the results presented demonstrate that nonlinear dynamics is a viable tool for analysing brake squeal data in order to provide improved understanding of the mechanism of brake squeal generation. Knowledge of routes to chaos, attractors and their underlying mechanisms could have potential application for the prediction of brake squeal propensity and its control. More insight could be gained by exploring further analytical models with dry friction and numerical simulation of a full brake system with nonlinear time series analysis of the sound pressure. Additional test data of a simplified brake system

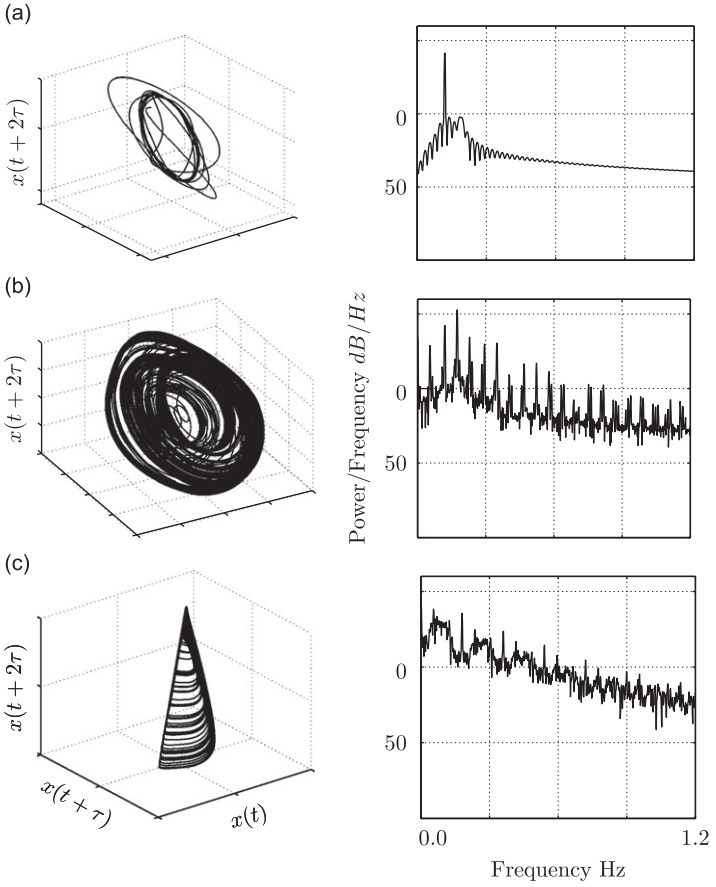

Fig. A1. Phase space plots and power spectral densities (PSD) for the 1-dof friction oscillator: (a) limit cycle; (b) torus; (c) chaotic regime.

and a full brake system in an industrial dynamometer with a high sampling rate, several accelerometers, laser vibrometer and microphones, and better-controlled parameters (constant pressure, specifically designed velocity regimes), would help to reveal more routes to chaos and, hence, brake squeal generation.

Acknowledgments

The first author (Oberst) acknowledges the receipt of a University of New South Wales University College Postgraduate Research Scholarship for the pursuit of this study. Also, the authors would like to thank PBR Pty. Ltd. and especially Dr. Antti Papinniemi, for the provision with measurement data from an industrial noise dynamometer.

Appendix A

A.1. Example of sinusoidally driven one degree-of-freedom friction oscillator

In this section, the nonlinear dynamics of a single dof friction oscillator, as shown in Fig. 1, and is examined. The governing equations are taken from [22].

$$m\ddot{x}(t)+c\dot{x}(t)+kx(t)=F_f(v_{\mathrm{rel}})+kA\cos\Omega t \tag{A.1}$$

$$v_{\mathrm{rel}}=v_0-v, \quad \text{with } F_f=-\mu(\mathrm{sgn}(v_{\mathrm{rel}}))F_n \tag{A.2}$$

The oscillator is excited by force, F, which acts through a spring of stiffness, k. The rotor is simulated by a moving plane in the form of a moving rigid surface. The mass, the spring's stiffness, the damping coefficient, friction and normal force and the friction coefficient are represented by m, k, c, F_f, F_n and μ respectively. With m = 1 kg, c = 0.1 Ns/m and k = 1 N/m, the frequency, f, and amplitude, A, of the exciting harmonic force, F, are set to f=0.1 Hz and A=3 N, respectively. Eq. (A.2) is important in the sense, that it represents the slip velocity and allows for a slip velocity of zero, back and forth switching between different systems of differential equations, a sticking and slipping state [108]. The belt's velocity is chosen as the bifurcation parameter and is varied from 15 to 10 and then 0.2 m/s to explore the ensuing motion. In the friction model used, μ decreases linearly with increasing relative velocity v_{rel}. The threshold value of the sticking regime is $\varepsilon=0.01$. If v_{rel} is less than ε the friction coefficient assumes its static value $\mu_s=0.7$; otherwise it is given by $\mu=\mu_s-\alpha v_{\mathrm{rel}}$ with $\mu_k=0.1$ as a lower bound. The kinetic friction coefficient becomes active when numerically $\mu<\mu_k$. The negative slope of the friction

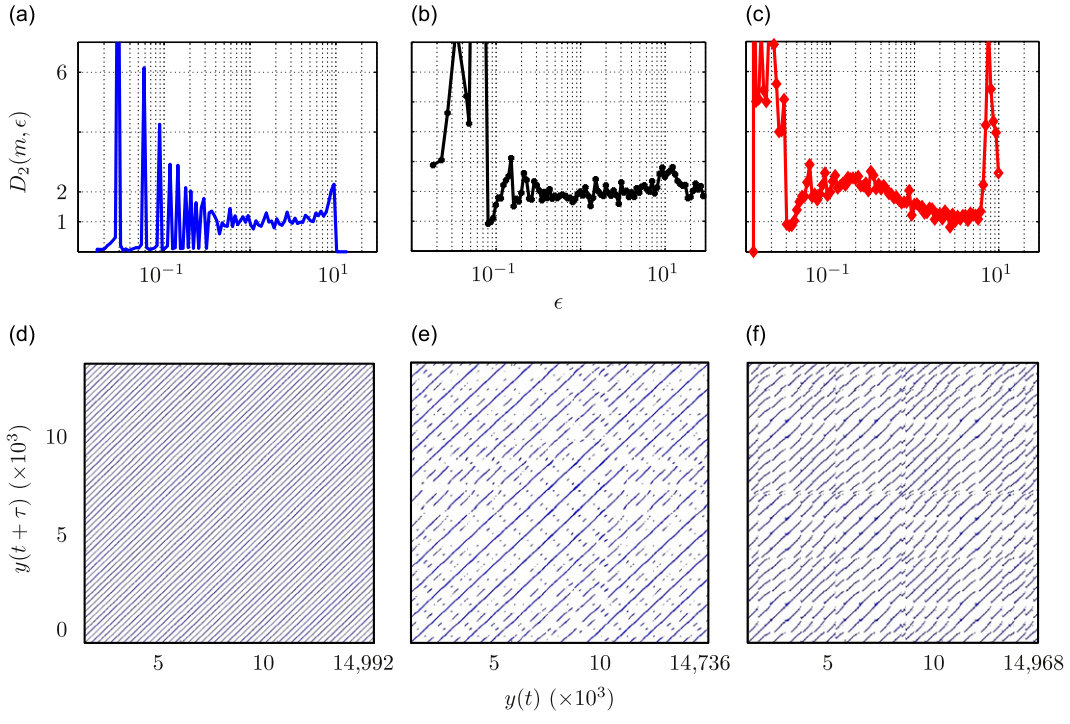

Fig. A2. Correlation dimension (D_2) for attractors: (a) limit cycle; (b) torus; (c) chaotic regime and recurrence plots (RP): (d) limit cycle; (e) torus; (f) chaotic attractor.

characteristic is given with $\alpha = 0.1$. As contact definition, a *continuous* representation is chosen rather than a *locking* formulation: No real sticking with a block velocity of zero is enforced in the sticking regime corresponding to creep-slip/microslip behaviour. When the relative velocity of pad and disc is less than the threshold value $\varepsilon = 0.01$, the velocity decreases prior to the default static value μ_s.

The phase space representation calculated from the time series data are shown in Fig. A1 together with the corresponding power spectrum. Different values v (15, 10 and 0.2 m/s) reveal three regimes: A limit cycle (one frequency); a weakly chaotic regime with a toroidal attractor (multiple distinct frequencies); and a broadband chaotic regime. This example shows the Ruelle–Takens–Newhouse route to chaos as also investigated by for instance Hinrichs et al. [22]. The correlation dimension D_2 of the three attractors, for the sake of illustration is presented as the average value of 20 dimensions in Fig. A2. The estimate of the fractal dimension is indicated by the horizontal part of the curves where less oscillations are present. In Fig. A2(a) scaling around D_2=1 becomes obvious which is indicative of the topological dimension of a limit cycle. In Fig. A2(b), a scaling around dimension two is visible and in Fig. A2(c) for small ε around 6×10^{-2}–4×10^{-1} a scaling above two is discernible. The high values of D_2 at very small length scales (ε) and large length scales are due to the discretization process and the finite length of the time series, respectively [81,82]. In Fig. A2, the *RPs* of the three regimes are presented. The periodic state in Fig. A2(d) shows straight lines. The RP of the weak chaotic torus in Fig. A2(e) shows generally long, straight and broken lines which indicate quasi-periodicity. However, the lines are broken and indicate unpredictability on another time scale. The chaotic regime in Fig. A2(f) shows different, changing regimes and, in general, shorter, broken lines which correspond to recurrent, though non-periodic and unpredictable, states.

References

[1] A. Akay, Acoustics of friction, *Journal of the Acoustical Society of America* 111 (4) (2002) 1525–1548.
[2] H. Abendroth, B. Wernitz, The integrated test concept: dyno-vehicle, performance-noise, SAE Technical Paper Series, 2000-01-2774, 2000.
[3] M. Yang, P. Blaschke, A.-H. Afaneh, A study of disc brake high frequency squeal and disc in-plane/out-of-plane modes. SEA Technical Papers, 2003-01-1621, 2003, pp. 1–8.
[4] N. Hinrichs, M. Oestreich, K. Popp, On the modelling of friction oscillators, *Journal of Sound and Vibration* 216 (3) (1998) 435–459.
[5] N.M. Kinkaid, O.M. O'Reilly, P. Papadopoulos, Automotive disc brake squeal, *Journal of Sound and Vibration* 267 (2003) 105–166.
[6] H. Ouyang, W. Nack, Y. Yuan, F. Chen, Numerical analysis of automotive disc brake squeal: a review, *International Journal of Vehicle Noise and Vibration* 1 (2005) 207–231.
[7] F. Chen, Automotive disk brake squeal: an overview, *International Journal of Vehicle Design* 51 (1/2) (2009) 39–72.
[8] S. Oberst, J.C.S. Lai, A critical review on brake squeal and its treatment in practice, *Internoise 2008*, Shanghai, China, 2008.
[9] N. Hoffmann, L. Gaul, Friction induced vibrations of brakes: research fields and activities, *SAE Technical Paper Series*, 2008-01-2579, 2008, pp. 1–8.
[10] F. Cramer, *Chaos and Order: Complex Structure of Living Systems*, Wiley VCH Verlagsgesellschaft, Weinheim, New York, 1993.
[11] H.G. Schuster, W. Just, *Deterministic Chaos: An Introduction*, Wiley VCH Verlagsgesellschaft, Weinheim-New York, 2005.
[12] S.J. Linz, J.C. Sprott, Elementary chaotic flow, *Physics Letters A* 259 (1999) 240–245.
[13] S.W. Shaw, On the dynamic response of a system with dry friction, *Journal of Sound and Vibration* 108 (2) (1986) 305–325.
[14] E. Ott, *Chaos in Dynamical Systems*, Cambridge University Press, GB, 1993.
[15] M. Kunze, T. Küpper, Qualitative bifurcation analysis of a non-smooth friction-oscillator model, *Zeitschrift für Angewandte Mathematik und Physik* 48 (1997) 87–101.
[16] M. Kunze, Non-smooth dynamical systems, Univerität Kóln, Habilitationsschrift, 1998.
[17] J. Awrejcewicz, P. Olejnik, Analysis of dynamic systems with various friction laws, *Applied Mechanics Reviews* 58 (November) (2005) 389–411.
[18] B. Erickson, B. Birnir, D. Lavallée, A model for aperiodicity in earthquakes, *Nonlinear Processes Geophysics* 15 (2008) 1–12.
[19] K. Popp, P. Stelter, Stick–slip vibrations and chaos, *Philosophical Transactions: Physical Sciences and Engineering* 332 (1624) (1990) 89–105.
[20] B.F. Feeny, F.C. Moon, Bifurcation sequences of a coulomb friction oscillator, *Nonlinear Dynamics* 4 (1992) 25–37.
[21] B. Feeny, F.C. Moon, Chaos in a forced dry-friction oscillator: experiments and numerical modelling, *Journal of Sound and Vibration* 170 (February) (1994) 303–323.
[22] N. Hinrichs, M. Oestreich, K. Popp, Dynamics of oscillators with impact and friction, *Chaos, Solitons & Fractals* 8 (4) (1997) 535–558.
[23] K. Shin, M.J. Brennan, J.-E. Oh, C.J. Harris, Analysis of disc brake noise using a two-degree-of-freedom model, *Journal of Sound and Vibration* 254 (5) (2002) 837–848.
[24] K. Shin, J.-E. Oh, M.J. Brennan, Nonlinear analysis of friction induced vibrations of a two-degree of freedom model for disc brake squeal, *JSME International Journal Series C* 45 (2002) 426–432.
[25] N. Hoffmann, M. Fischer, R. Allgaier, L. Gaul, A minimal model for studying properties of the mode-coupling type instability in friction induced oscillations, *Mechanics Research Communications* 29 (2002) 197–205.
[26] O. Giannini, A. Akay, F. Massi, Experimental analysis of brake squeal noise on a laboratory brake setup, *Journal of Sound and Vibration* 292 (2006) 1–20.
[27] A. Buck, Simulation von Bremsenquietschen (Brake Squeal), PhD Thesis, Lehrstuhl für Baumechanik, Technische Universität München, 2008.
[28] G.G. Adams, Self-excited oscillations of two elastic half-spaces sliding with a constant coefficient of friction, *ASME Journal of Applied Mechanics* 62 (1995) 867–872.
[29] G.G. Adams, Steady sliding of two elastic half-spaces with friction reduction due to interface stick–slip, *ASME Journal of Applied Mechanics* 65 (1998) 470–475.
[30] L. Baillet, S. D'Errico, Y. Berthier, Influence of sliding contact local dynamics on macroscopic friction coefficient variation, *Revue europeenne des elements finis* 10 (2005) 1–16.
[31] H.R. Mills, Brake squeak, Technical Report, The Institution of Automobile Engineers, Research Report, 9000 B and 9162 B, 1938.
[32] J.J. Thomson, Using fast vibrations to quench friction-induced oscillations, *Journal of Sound and Vibration* 228 (5) (1999) 1079–1102.
[33] A. Bajer, V. Belsky, S. Kung, The influence of friction-induced damping and nonlinear effects on brake squeal analysis, SAE Technical Paper, 2004-01-2794, 2004, pp. 1–9.
[34] G.X. Chen, Z.R. Zhou, P. Kapsa, L. Vincent, Experimental investigation into squeal under reciprocating sliding, *Tribology International* 36 (2003) 961–971.
[35] D.M. Beloiu, R.A. Ibrahim, Brake squeal as dynamic instability: an experimental investigation, *Structural Control and Health Monitoring* 13 (2006) 277–300.
[36] G.X. Chen, Z.R. Zhou, Time-frequency analysis of friction-induced vibration under reciprocating sliding conditions, *Wear* 262 (2007) 1–10.
[37] D. Stanef, A. Papinniemi, J. Zhao, From protoype to production—the practical nature of brake squeal noise, SAE Technical Paper Series, 2006-01-3217, 2006, pp. 1–10.
[38] P. Duffour, J. Woodhouse, Instability with frictional point contact. Part 3: experimental tests, *Journal of Sound and Vibration* 304 (2007) 186–200.

[39] M.T. Bengisu, A. Akay, Stability of friction-induced vibrations in multi-degree-of-freedom systems, *Journal of Sound and Vibration* 171 (4) (1994) 557–570.
[40] R.A. AbuBaker, H. Ouyang, A prediction methodology of disk brake squeal using complex eigenvalue analysis, *International Journal of Vehicle Design* 46 (2008) 416–435.
[41] F. Massi, L. Baillet, O. Giannini, A. Sestieri, Brake squeal: linear and nonlinear numerical approaches, *Mechanical Systems and Signal Processing* 21 (2007) 2374–2393.
[42] J. Jerrelind, A. Stenson, Nonlinear dynamics of parts in engineering systems, *Chaos, Solitons & Fractals* 11 (2000) 2413–2428.
[43] O. Giannini, A. Sestrieri, Predictive model of squeal noise occurring on a laboratory brake, *Journal of Sound and Vibration* 296 (2006) 583–601.
[44] G.X. Chen, Q.Y. Liu, X.S. Jin, Z.R. Zhou, Stability analysis of a squealing vibration model with time delay, *Journal of Sound and Vibration* 311 (2008) 516–536.
[45] K. Popp, Modelling and control of friction-induced vibrations, *Mathematical and Computer Modelling of Dynamical Systems* 11 (3) (2005) 345–369.
[46] P. Kowalczyk, Robust chaos and border-collision bifurcations in non-invertible piecewise-linear maps, *Nonlinearity* 18 (2005) 485–504.
[47] A. Tuchinda, N.P. Hoffmann, D.J. Ewins, W. Keiper, Mode lock-in characteristics and instability study of the pin-on-disc system, *Proceedings of the International Modal Analysis Conference*, IMAC XX, Kissimee, vol. 1, 2001, pp. 71–77.
[48] N. Coudeyras, J.-J. Sinou, Nacivet, A new treatment of predicting the self-excited vibrations of nonlinear systems with frictional interfaces: the constrained harmonic balance method, with application to disc brake squeal, *Journal of Sound and Vibration* 319 (2009) 1175–1199.
[49] N. Coudeyras, S. Nacivet, J.-J. Sinou, Periodic and quasi-periodic solutions for multi-instabilities involved in brake squeal, *Journal of Sound and Vibration* 328 (2009) 520–540.
[50] G.X. Chen, Z.R. Zhou, A self-excited vibration model based on special elastic vibration mode of friction systems and time delays between the normal and friction forces: a new mechanism for squealing noise, *Wear* 262 (2007) 1123–1239.
[51] N. Hoffmann, L. Gaul, A sufficient criterion for the onset of sprag-slip oscillations, *Archive of Applied Mechanics* 73 (2004) 650–660 10.1007/S00419-033-0315-4.
[52] H. Ouyang, J.E. Mottershead, M.P. Cartmell, D.J. Brookfield, Friction-induced vibraion of an elastic slider on a vibrating disc, *International Journal of Mechanical Science* 41 (1999) 325–336.
[53] N. Hoffmann, L. Gaul, Effects of damping on mode-coupling instability in friction induced oscillations, *Zeitschrift für Angewandte Mathematik und Mechanik* 83 (8) (2003) 524–534.
[54] O. Giannini, A. Sestieri, F. Massi, A. Akay, Experimental investigation and modeling of brake squeal using simplified test rigs, SAE Technical Paper Series, 2007-01-3963, 2007, pp. 189–200.
[55] F. Massi, O. Giannini, L. Baillet, Brake squeal as dynamic instability: an experimental investigation, *Journal of the Acoustical Society of America* 120 (3) (2006) 1388–1398.
[56] F. Massi, F. Giannini, Effect of damping on the propensity of squeal instability: an experimental investigation, *Journal of Acoustical Society of America* 123 (2008) 2017–2023.
[57] B. Hervé, J.-J. Sinou, H. Mahé, L. Jézéquell, Analysis of squeal noise and mode coupling instabilities including damping and gyroscopic effects, *European Journal of Mechanics A/Solids* 27 (2008) 141–160.
[58] B. Hervé, J.J. Sinou, H. Mahé, L. Jézéquell, Extension of the destabilization paradox to limit cycle amplitudes for a nonlinear self-excited system subject to gyroscopic and circulatory actions, *Journal of Sound and Vibration* 323 (2009) 944–973.
[59] B.F. Feeny, F.C. Moon, Quenching stick–slip chaos with dither, *Journal of Sound and Vibration* 237 (1) (2000) 173–180.
[60] F. Chen, A. Wang, C.A. Tan, Dynamic system instability suppression with dither technique, *Proceedings of the 22nd SAE Brake Colloquium*, Anaheim, CA, USA, 2004.
[61] M. Paliwal, A. Mahajan, T. Don, J. Chu, P. Filip, Noise and vibration analysis of a disc-brake system using a stick–slip friction model involving coupling stiffness, *Journal of Sound and Vibration* 282 (2002) 1273–1284.
[62] H. Hetzler, D. Schwarzer, W. Seemann, Analytical investigation of steady-state stability and hopf-bifurcations occurring in sliding friction oscillators with application to low-frequency disc brake noise, *Communications in Nonlinear Science and Numerical Simulations* 12 (2007) 83–99.
[63] H. Ouyang, Assignment of complex eigenvalues to second-order damped asymmetric systems through state-feedback, *NOVEM2009*, 5–8 April, Oxford, England, 2009.
[64] H. Ouyang, L. Baeza, S. Hu, A receptance-based method for predicting latent roots and critical points in friction-induced vibration problems of asymmetric systems, *Journal of Sound and Vibration* 321 (2009) 1058–1068.
[65] F.P. Bowden, L. Leben, Nature of sliding and the analysis of friction, *Nature* 3572 (1938) 691–692.
[66] F.P. Bowden, D. Tabor, Mechanism of metallic friction, *Nature* 3798 (1942) 197–199.
[67] S.W.E. Earles, G.B. Soar, Squeal noise in disc brakes, in: *Vibration and Noise in Motor Vehicles*, Institution of Mechanical Engineers, C 101/71, 1971, pp. 61–69.
[68] S.W.E. Earles, A mechanism of disc-brake squeal, SEA Technical Papers, 770181, 1978, pp. 1–6.
[69] S.W.E. Earles, M.N.M. Badi, Oscillatory instabilities generated in a double-pin and disc undamped system: a mechanism of disc-brake squeal, *Proceedings of the Institution of Mechanical Engineers, Part C: Mechanical Engineering Science* 198 (4) (1984) 43–49.
[70] S.W.E. Earles, P.W. Chamber, Disc brake squeal noise generation: predicting its dependency on system parameters including damping, *International Journal of Vehicle Design* 8 (4/5/6) (1987) 538–552.
[71] W.W. Tworzydlo, O.N. Hamzeh, W. Zaton, T.J. Judek, Friction-induced oscillations of a pin-on-disk slider: analytical and experimental studies, *Wear* 236 (1999) 9–23.
[72] P. Duffour, J. Woodhouse, Instability of systems with a frictional point contact. Part 1: basic modelling, *Journal of Sound and Vibration* 271 (2004) 365–390.
[73] P. Duffour, J. Woodhouse, Instability of systems with a frictional point contact. Part 2: model extensions, *Journal of Sound and Vibration* 271 (2004) 301–410.
[74] T. Butlin, J. Woodhouse, Sensitivity of friction-induced vibration in idealized systems, *Journal of Sound and Vibration* 319 (2009) 182–198.
[75] J.H. Tarter, Disc brake squeal, SAE Technical Paper, 830530, 1983, pp. 1–8.
[76] M. Suganami, M. Nakai, M. Yokoi, T. Miyahara, H. Matsui, I. Yamazaki, Disk brake squeal by a model of a rotating disk and a beam, *Proceedings of the First International Symposium on Impact and Friction of Solids*, *Structures and Intelligent Machines*, Congress Center, Ottawa, Canada, 1998.
[77] A. Akay, J.A. Wickert, Z. Xu, Investigation of mode lock-in and friction interface, Technical Report, Final Report, Department of mechanical engineering, Carnegie Mellon University, 2000.
[78] O. Giannini, F. Massi, Characterization of the high-frequency squeal on a laboratory brake setup, *Journal of Sound and Vibration* 310 (2008) 394–408.
[79] F. Massi, Dynamic and Tribological Analysis of Brake Squeal, PhD Thesis, University of Rome "la Sapieza", Italy, 2006.
[80] F. Massi, Y. Berthier, L. Baillet, Contact surface topography and system dynamics of brake squeal, *Wear* 265 (2008) 1784–1792.
[81] J.C. Sprott, *Chaos and Time-series Analysis*, Oxford University Press, Oxford, New York, 2003.
[82] H. Kantz, T. Schreiber, *Nonlinear Time Series Analysis*, Cambridge University Press, Cambridge, 2004.
[83] J. Stark, D.S. Broomhead, M.E. Daview, J. Huke, Takens embedding theorems for forced and stochastic systems, *Nonlinear Analysis, Theory, Methods & Applications* 30 (8) (1997) 5303–5314.
[84] J.M. Martinerie, A.M. Albano, A.I. Mees, P.E. Rapp, Mutual information strange attractors, and the optimal estimation of dimension, *Physical Review A* 45 (10) (1992) 7058–7064.
[85] N. Marwan, J. Kurths, P. Saparin, Generalised recurrence plot analysis for spatial data, *Physics Letters A* 360 (2007) 545–551.
[86] R. Gilmore, M. Lefranc, *Topology Analysis of Chaos*, Wiley VCH Verlagsgesellschaft, 2002.
[87] P. Grassberger, I. Procaccia, Characterization of strange attractors, *Physical Review Letters* 50 (5) (1983) 346–349.

[88] F.C. Moon, *Chaotic and Fractal Dynamics*, John Wiley & Sons, New York, Chichester, Brisbane, Toronto, Singapore, 1992.
[89] Ya.B. Pesin, Characteristic Lyapunov exponents and smooth ergodic theory, *Russian Mathematical Surveys* 32 (4) (1977) 55–114.
[90] N. Marwan, M. Carmen Romano, M. Thiel, J. Kurths, Recurrence plots for the analysis of complex systems, *Physics Reports* 438 (2007) 237–329.
[91] J.-P. Eckmann, D. Ruelle, Ergodic theory of chaos and strange attractors, *The American Physical Society* 57 (3) (1985) 617–656.
[92] M.C. Romano Blasco, Synchronization Analysis by Means of Recurrences in Phase Space, PhD Thesis, Mathematisch-Naturwissenschaftliche Fakultät/Universität Potsdam, 2004.
[93] N. Marwan, M.H. Trauth, M. Vuille, J. Kurths, Comparing modern and pleistocene ENSO-like influences in NW Argentina using nonlinear time series analysis methods, *Climate Dynamics* 21 (2003) 317–326.
[94] M. Thiel, Exploiting Naturally Occurring Analogues, PhD Thesis, Universität Potsdam, Mathematisch-Naturwissenschaftliche Fakultät, 2004.
[95] F. Chen, F. Tan, C. Chen, C.A. Tan, R.L. Quaglia, Disc brake squeal: mechanism, analysis, evaluation and reduction/prevention, SAE-Society of Automotive Engineers, 2006.
[96] S. Moore, J.C.S. Lai, S. Oberst, A. Papinniemi, Z. Hamdi, D. Stanef, Design of experiments in brake squeal, *Internoise 2008*, Shanghai, China, 2008.
[97] J. Flint, J. Hald, Traveling waves in squealing disc brakes measured with acoustic holography. SEA Technical Papers, 2003-01-3319, 2003, pp. 1–8.
[98] Surface vehicle recommended practice, disc and drum brake dynamometer squeal noise matrix, Technical Report, SAE J2521, 2006.
[99] L.L. Trulla, A. Giuliani, J.P. Zbilut, C.L. Webber Jr., Recurrence quantification analysis of the logistic equation with transients, *Physical Letters A* 223 (4) (1996) 255–260.
[100] R. Hegger, H. Kantz, T. Schreiber, Practical implementation of nonlinear time series methods: the [small-caps TISEAN] package, *Chaos: An Interdisciplinary Journal of Nonlinear Science* 9 (2) (1999) 413–435.
[101] H. Kantz, T. Schreiber, I. Hoffmann, T. Buzug, G. Pfister, L.G. Flepp, J. Simonet, R. Badii, E. Brun, Nonlinear noise reduction: a case study on experimental data, *Physical Review E* 48 (2) (1993) 1529–1538.
[102] P. Grassberger, R. Hegger, H. Kantz, C. Schaffrath, T. Schreiber, On noise reduction methods for chaotic data, *Chaos: An Interdisciplinary Journal of Nonlinear Science* 3 (2) (1993) 127–141.
[103] N. Marwan, N. Wessel, A. Meyerfeldt, A. Schirdewan, J. Kurths, Recurrence plot based measures of complexity and its application to heart rate variability data, *Physical Review E* 2 (026702) (2002) 1–8.
[104] J. Guckenheimer, P. Holmes, *Nonlinear Oscillations, Dynamical Systems, and Bifurcations of Vector Fields*, vol. 42, Springer-Verlag, Berlin, New York, 1997.
[105] H. Kantz, A robust method to estimate the maximal Lyapunov exponent of a time series, *Physical Letters A* 185 (1) (1994) 77–87.
[106] S. Oberst, J.C.S. Lai, Numerical study of friction-induced pad-mode instability in disc brake squeal, *20th International Congress on Acoustics* (*ICA 2010*), 23–27 August, Sydney, Australia, 2010.
[107] S. Oberst, J.C.S. Lai, Acoustic radiation of friction-induced pad-mode instability in disc brake squeal, *20th International Congress on Acoustics* (*ICA 2010*), 23–27 August, Sydney, Australia, 2010.
[108] R.I. Leine, D.H. Van Campen, B.L. Van De Vrande, Bifurcations in nonlinear discontinuous systems, *Nonlinear Dynamics* 23 (2000) 105–164.